Two Anhydrous Zeolite X Crystal Structures, $Ca_{31}Rb_{30}Si_{100}Al_{92}O_{384}$ and $Ca_{28}Rb_{36}Si_{100}Al_{92}O_{384}$

Se Bok Jang, Mi Sook Kim, Young Wook Han*, and Yang Kim

Department of Chemistry, Pusan National University, Pusan 609-735, Korea
**Department of Science Education, Pusan National University of Education, Pusan 607-736, Korea*
Received March 12, 1996

The structures of fully dehydrated Ca^{2+}- and Rb^+-exchanged zeolite X, $Ca_{31}Rb_{30}Si_{100}Al_{92}O_{384}$ ($Ca_{31}Rb_{30}$-X; $a=25.009(1)$ Å) and $Ca_{28}Rb_{36}Si_{100}Al_{92}O_{384}$ ($Ca_{28}Rb_{36}$-X; $a=24.977(1)$ Å), have been determined by single-crystal X-ray diffraction methods in the cubic space group $Fd\bar{3}$ at 21(1) ℃. Their structures were refined to the final error indices $R_1=0.048$ and $R_2=0.041$ with 236 reflections for $Ca_{31}Rb_{30}$-X, and $R_1=0.052$ and $R_2=0.043$ with 313 reflections for $Ca_{28}Rb_{36}$-X; $I>3\sigma(I)$. In both structures, Ca^{2+} and Rb^+ ions are located at six different crystallographic sites. In dehydrated $Ca_{31}Rb_{30}$-X, sixteen Ca^{2+} ions fill site I, at the centers of the double 6-rings (Ca-O=2.43(1) Å and O-Ca-O=93.3(3)°). Another fifteen Ca^{2+} ions occupy site II (Ca-O=2.29(1) Å, O-Ca-O=119.5(5)°) and fifteen Rb^+ ions occupy site II opposite single six-rings in the supercage; each is 1.60 Å from the plane of three oxygens (Rb-O=2.77(1) and O-Rb-O=91.1(4)°). About two Rb^+ ions are found at site II', 1.99 Å into sodalite cavity from their three-oxygen plane (Rb-O=2.99(1) Å and O-Rb-O=82.8(4)°). The remaining thirteen Rb^+ ions are statistically distributed over site III, a 48-fold equipoint in the supercages on twofold axes (Rb-O=3.05(1) Å and Rb-O=3.38(1) Å). In dehydrated $Ca_{28}Rb_{36}$-X, sixteen Ca^{2+} ions fill site I (Ca-O=2.41(1) Å and O-Ca-O=93.6(3)°) and twelve Ca^{2+} ions occupy site II (Ca-O=2.31(1) Å, O-Ca-O=119.7(4)°). Sixteen Rb^+ ions occupy site II; each is 1.60 Å from the plane of three oxygens (Rb-O=2.81(1) and O-Rb-O=90.6(3)°) and four Rb^+ ions occupy site II'; each is 1.88 Å into sodalite cavity from their three-oxygen plane (Rb-O=2.99(1) and O-Rb-O=83.8(2)°). The remaining sixteen Rb^+ ions are found at III site in the supercage (Rb-O=2.97(1) Å and Rb-O=3.39(1) Å). It appears that Ca^{2+} ions prefer sites I and II in that order, and that Rb^+ ions occupy the remaining sites. Rb^+ ions are too large to be stable at site I, when they are competing with other smaller cations like Ca^{2+} ions.

Introduction

The properties of zeolites are sensitive to their cationic contents. A knowledge of the siting of these cations within a zeolite framework can provide a structural basis for understanding these properties. The thermal stability, sorption parameters, and catalytic properties of zeolites are all determined by the type and number of exchangeable cations and their distribution over the available sites. Cation distributions in faujasite-type zeolites have been widely studied by X-ray diffraction methods.[1~3]

Recent single-crystal X-ray studies of hydrated chabazite[4~6] and heulandite,[7] exchanged under controlled conditions with mono- and divalent cations, have shown that the extra-framework structures, especially the cation distributions, may be rationalized to a large extent in terms of the sizes, charges, and electronic natures of the exchanged cations. In addition, these studies have shown that the comparison of the electron density maps of the same zeolite, exchanged with different cations, may be useful in determining site locations and possibly the approximate ratio of two different cations at the same site.

Smolin, Shepelev, and Anderson studied the crystal structures of hydrated and dehydrated Ca^{2+}-exchanged zeolite X.[8] They also investigated the migration of cations during dehydration by heating the crystal in a stream of hot N_2 gas. In the initial hydrated form, Ca^{2+} ions are located in the sodalite cavities and supercages. Upon dehydration, the Ca^{2+} ions migrate into the hexagonal prism and to sites in the single six-oxygen rings.

Shepelev, Butikova and Smolin studies the crystal structures of the partially K^+-, Rb^+-, and Cs^+- exchanged forms of NaX zeolite in both the hydrated and the dehydrated (400 ℃) states.[9] They investigated the migration of cations during the dehydration. Analysis of the cation distribution in the hydrated forms shows that K^+ ions penetrate into all zeolite cavities, whereas Rb^+ ions diffuse into the sodalite cage, but not into the hexagonal prism, and Cs^+ ions are located only in the supercage. Dehydration of the zeolites is accompanied by a migration of unexchanged sodium cations into the hexagonal prism. Destruction of the dehydrated Rb^+-exchanged crystal after the 6 hour-long exposure at 400 ℃ seems to be caused by a slow migration of the Rb^+ ions into the hexagonal prism.

In our recent work, the crystal structure of dehydrated Ca^{2+} and K^+-exchanged zeolite X, $Ca_{32}K_{28}$-X, has been determined[10] by single-crystal X-ray diffraction methods.[10] In this structure, the principal positions of Ca^{2+} ion are the positions at site I, the center of the double six-oxygen ring (symmetry of $\bar{3}$) and also the positions at site II in the supercage, symmetry of 3. Because the ionic radius of K^+ ion is larger than that of Ca^{2+} ion, large K^+ ions preferentially occupy sites II and III, deep in the large supercage. Smaller Ca^{2+} ions occupy smaller pore sites such as the centers of the double 6-rings and the positions near the centers of single 6-ring planes in the supercage.

The present study has been initiated to investigate the site selectivity of cations in the crystal structure of Ca^{2+}

and Rb^+ exchanged zeolite X. It would be interesting to learn how different numbers of exchanged Ca^{2+} ions (divalent cation) and Rb^+ ions (monovalent cation) arrange themselves in the zeolite framework. In addition, the site selectivities for these two ions of substantially different size and charge would be studied. Because their scattering factors and ionic radii are quite different, reliable and precise structures of Ca^{2+} and Rb^+ exchanged zeolite X can be determined by X-ray crystallography.

Experimental Section

Large colorless crystals of Na-X (stoichiometry; $Na_{92}Si_{100}Al_{92}O_{384}$) were prepared in St. Petersburg, Russia.[11] Each of two single crystals, a colorless octahedron *ca.* 0.25 mm in cross-section, was lodged in a fine Pyrex capillary.

$Ca_{31}Rb_{30}$-X and $Ca_{28}Rb_{36}$-X were prepared using an exchange solutions whose $Ca(NO_3)_2 : RbNO_3$ mole ratios were 1 : 1 and 1 : 100, respectively, with a total concentration of 0.05 M. Ion exchange was accomplished by flow methods: each aqueous solution was allowed to flow past each crystal at a velocity of approximately 1.5 cm/s for three days at 24(1) ℃. Each capillary with its crystal was then connected to a vacuum line. Each crystal was cautiously dehydrated under vacuum by gradually increasing its temperature (*ca.* 20 ℃/h) to 380 ℃ at a constant pressure of 2×10^{-6} Torr. These conditions were maintained for 48 h. After each crystal had cooled to room temperature, it was sealed under vacuum in its capillary by torch. Both crystals had become pale yellow.

X-ray Data Collection

Preliminary crystallographic experiments and subsequent data collection were performed with an automated four-circle Enraf-Nonius CAD-4 diffractometer equipped with a graphite monochromator, a pulse-height analyzer and a micro-Vax 3100 computer. Mo Kα radiation (Kα1, $\lambda=0.70930$ Å; Kα2, $\lambda=0.71359$ Å) was used for all experiments. The cubic unit cell constants determined by a least-squares refinement of 25 intense reflections for which $14°<2\theta<24°$ are 25.009(1) Å for $Ca_{31}Rb_{30}$-X and 24.977(1) Å for $Ca_{28}Rb_{36}$-X.

For each crystal, the ω-2 scan technique was used. The data were collected at variable scan speeds. Most reflections were observed at slow speeds from 0.24 to 0.34 degree/min in ω. The intensities of three reflections in diverse regions of reciprocal space were recorded every three hours to monitor crystal and instrument stability. Only small random fluctuations of these check reflections were noted during the course of data collection. All unique reflections for an F-centered unit cell for which $2\theta<60°$ for each crystal was examined by counter methods.

The raw data were corrected for Lorentz and polarization effects including incident beam monochromatization, and the resultant estimated standard deviations were assigned to each reflection by the computer programs PROCESS and GENESIS.[12] Of the 1249 unique reflections measured for $Ca_{31}Rb_{30}$-X and 1248 for $Ca_{28}Rb_{36}$-X, only the 236 and 313 reflections, respectively, for which $I>3\sigma(I)$ were used in subsequent structure determinations.

Structure Determination

The crystal structures were solved in the cubic space group $Fd\bar{3}$. This is established for zeolite X, and is consistent with the systematic absences observed.

$Ca_{31}Rb_{30}$-X. Full-matrix least-squares refinement was initiated using the atomic parameters of the framework atoms [Si, Al, O(1), O(2), O(3), and O(4)] of dehydrated Na-X treated with Rb vapor.[13] Anisotropic refinement of the framework atoms converged to an unweighted R_1 index, $(\Sigma(|F_o|-|F_c||)/\Sigma F_o)$, of 0.32 and a weighted R_2 index, $(\Sigma w(F_o-|F_c|)^2/\Sigma wF_o^2)^{1/2}$, of 0.38. The initial difference Fourier function revealed two large peaks: at (0.0, 0.0, 0.0) with peak height 10.0 eÅ^{-3}, and at (0.254, 0.254, 0.254) with peak height 5.4 eÅ^{-3}. These two positions were stable in least-squares refinement. Anisotropic refinement of framework atoms and isotropic refinement of Ca(1) and Rb(2) converged to $R_1=0.156$ and $R_2=0.166$ with occupancies Ca(1)=10.9(6) and Rb(2)=16.5(5).

It is not difficult to distinguish Ca^{2+} from Rb^+ ions for several reasons. Firstly, their atomic scattering factors are quite different, 18 e^- for Ca^{2+} *vs.* 36 e^- for Rb^+. Secondly, their ionic radii are different, $Ca^{2+}=0.99$ Å and $Rb^+=1.47$ Å.[14] Also, the approach distances between Ca^{2+} and zeolite oxygens have been determined in the previous structure (Ca_{46}-X)[10] and are indicative. Finally, the requirement that the cationic charges sum to +92 per unit cell does not allow the major positions to refine to acceptable occupancies with an alternative assignment of ionic identities.

A subsequent difference Fourier function revealed two additional peaks: at (0.416, 0.125, 0.125) with height 2.8 eÅ^{-3}, and at (0.210, 0.210, 0.210) with height 1.9 eÅ^{-3}. Inclusion of these peaks as ions at Rb(3) and Ca(2) lowered the error indices to $R_1=0.052$ and $R_2=0.049$ (see Table 1). The occupancy numbers at Rb(3) and Ca(2) refined to 13.9(3) and 20.3(4), respectively.

From successive difference Fouriers, one peak was found at (0.170, 0.170, 0.170) with height 1.2 eÅ^{-3}. Anisotropic refinement of framework atoms and all the cations converged to $R_1=0.045$ and $R_2=0.039$. The occupancies of Ca(1), Ca(2), Rb(1), Rb(2), and Rb(3) were fixed at the values shown in Table 1 considering the cationic charge per unit cell. The sum of occupancy numbers at Ca(2), Rb(1), and Rb(2) were fixed at 32.0, the maximum number of ions per unit cell at these positions. Otherwise unacceptablely close intercationic distances would occur. The final error indices were $R_1=0.048$ and $R_2=0.041$. The shifts in the final cycle of least-squares refinement were less than 0.1% of their corresponding standard deviations. The final difference function was featureless except for a peak of height 0.81 eÅ^{-3} at (0.082, 0.082, 0.668). This peak was not within bonding distance of any other atom, and was not considered further.

An absorption correction ($\mu R=0.341$, $\rho_{cal}=1.619$ g/cm^3, F(000)=7352)[15] was made empirically using a Ψ scan. The adjusted transmission coefficients ranged from 0.993 to 0.999. This correction had little effect on the final R values. The final structure parameters and selected interatomic distances and angles are presented in Tables 1 and 2, respectively.

$Ca_{28}Rb_{36}$-X. Full-matrix least-squares refinement was initiated by using the atomic parameters of framework atoms

Table 1. Positional, thermal[a], and occupancy parameters

a. dehydrated $Ca_{31}Rb_{30}$-X

Atom	Wyc. Pos.	x	y	z	[b]β_{11}	β_{22}	β_{33}	β_{12}	β_{13}	β_{23}	Occupancy[c] varied	fixed
Si	96(g)	−540(2)	336(2)	1221(3)	3(1)	2(1)	2(1)	−2(2)	−1(2)	−6(2)		96
Al	96(g)	−558(2)	1221(3)	368(2)	4(1)	3(1)	3(1)	−1(2)	2(2)	0(2)		96
O(1)	96(g)	−1075(4)	−20(6)	1125(4)	10(3)	12(3)	1(2)	−6(5)	2(3)	−2(4)		96
O(2)	96(g)	−61(5)	−35(5)	1431(3)	5(2)	6(2)	3(2)	7(4)	−12(4)	−1(4)		96
O(3)	96(g)	−361(3)	615(4)	660(4)	6(2)	−3(2)[d]	4(2)	1(4)	4(4)	1(3)		96
O(4)	96(g)	−635(4)	772(5)	1701(4)	7(2)	8(2)	0(2)	−1(5)	8(4)	−4(3)		96
Ca(1)	16(c)	0	0	0	3(1)	3(1)	3(1)	1(2)	1(2)	1(2)	15.7(2)	16
Ca(2)	32(e)	2213(4)	2213(4)	2213(4)	14(1)	14(1)	14(1)	22(4)	22(4)	22(4)	15.1(3)	15
Rb(1)	32(e)	1730(10)	1730(10)	1730(10)	9(4)	9(4)	9(4)	0(10)	0(10)	0(10)	2.4(2)	2
Rb(2)	32(e)	2538(2)	2538(2)	2538(2)	12(1)	12(1)	12(1)	6(2)	6(2)	6(2)	14.9(1)	15
Rb(3)	48(f)	4160(5)	1250	1250	10(2)	28(3)	32(4)	0	0	−21(6)	12.8(2)	13

b. dehydrated $Ca_{28}Rb_{36}$-X

Atom	Wyc. Pos.	x	y	z	[b]β_{11}	β_{22}	β_{33}	β_{12}	β_{13}	β_{23}	Occupancy[c] varied	fixed
Si	96(g)	−545(2)	343(2)	1224(2)	5(1)	3(1)	2(1)	2(1)	−1(2)	−1(2)		96
Al	96(g)	−551(2)	1224(2)	357(2)	3(1)	2(1)	3(1)	−0(1)	−0(2)	2(2)		96
O(1)	96(g)	−1090(3)	−6(5)	1118(3)	4(2)	11(2)	4(2)	−3(3)	3(2)	−9(3)		96
O(2)	96(g)	−45(4)	−56(4)	1422(3)	7(2)	2(1)	3(2)	−0(34)	6(3)	−6(3)		96
O(3)	96(g)	−363(3)	624(4)	642(3)	7(2)	3(2)	1(2)	3(3)	2(3)	1(3)		96
O(4)	96(g)	−641(3)	784(4)	1690(4)	8(2)	5(2)	1(1)	−5(4)	9(3)	−4(2)		96
Ca(1)	16(c)	0	0	0	2(1)	2(1)	2(1)	0(1)	0(1)	0(1)	16.2(2)	16
Ca(2)	32(e)	2203(4)	2203(4)	2203(4)	10(2)	10(2)	10(2)	11(3)	11(3)	11(3)	11.6(3)	12
Rb(1)	32(e)	1735(6)	1735(6)	1735(6)	16(2)	16(2)	16(2)	−3(6)	−3(6)	−3(6)	4.0(2)	4
Rb(2)	32(e)	2544(1)	2544(1)	2544(1)	10(1)	10(1)	10(1)	2(1)	2(1)	2(1)	15.8(2)	16
Rb(3)	48(f)	4140(3)	1250	1250	6(1)	24(2)	29(2)	0	0	−17(4)	16.1(2)	16

[a]Positional and anisotropic thermal parameters are given×10^4. Numbers in parentheses are the esd's in the units of the least significant digit given for the corresponding parameter. [b]The anisotropic temperature factor=$\exp[-(\beta_{11}h^2+\beta_{22}k^2+\beta_{33}l^2+\beta_{12}hk+\beta_{13}hl+\beta_{23}kl)]$. [c]Occupancy factors are given as the number of atoms or ions per unit cell. [d]This physically unacceptable value was increased by 2σ in the preparation of Figures 2 and 3.

for the previous crystal of $Ca_{31}Rb_{30}$-X. Anisotropic refinement of the framework atoms converged to $R_1=0.35$ and $R_2=0.42$. A subsequent Fourier synthesis revealed two large peaks: at (0.0, 0.0, 0.0) with height 18.4 eÅ^{-3} and (0.253, 0.253, 0.253) with height 12.4 eÅ^{-3}. Anisotropic refinement of the framework atoms, Ca^{2+} at Ca(1), and Rb^+ at Rb(2) converged to $R_1=0.178$ and $R_2=0.200$ with occupancies of 9.9(6) at Ca(1) and 13.1(5) at Rb(2).

A subsequent difference Fourier function revealed two additional peaks: at (0.416, 0.125, 0.125) with height 3.70 eÅ^{-3}, and at (0.221, 0.221, 0.221) with height 3.52 eÅ^{-3}. Inclusion of these peaks as ions at Ca(2) and Rb(3) lowered the error indices to $R_1=0.073$ and $R_2=0.067$. The occupancy numbers at Ca(2) and Rb(3) refined to 18.0(3) and 12.3(4), respectively. The third Rb^+ ion position was found on an ensuing Fourier function at (0.175, 0.175, 0.175) with height 2.05 eÅ^{-3}. Anisotropic refinement of framework atoms and all the cations converged to $R_1=0.051$ and $R_2=0.041$. The occupancies of Ca(1), Ca(2), Rb(1), Rb(2), and Rb(3) were fixed at the values shown in Table 1 considering the cationic charge per unit cell. The final error indices were $R_1=0.052$ and $R_2=0.043$. The shifts in the final cycle of least-squares refinement were less than 0.1% of their corresponding standard deviations. The final difference function was featureless except for a peak of height 0.81 eÅ^{-3} at (0.125, 0.125, 0.125). This peak was not within bonding distance of any other atom, and was not considered further.

An absorption correction ($\mu R=0.394$, $\rho_{cal}=1.667$ g/cm^3, F(000)=7514)[13] was made empirically using a Ψ scan. The adjusted transmission coefficients ranged from 0.992 to 0.998. This correction had no effect on the final R indices.

All crystallographic calculations were done using MolEN[12] (a structure determination program package supplied by Enraf-Nonius). The full-matrix least-squares program used minimized $\Sigma w(F_o-|F_c|)^2$; the weight (w) of an observation was the reciprocal square of $\sigma(F_o)$, its standard deviation. Atomic scattering factors[16,17] for Si, Al, O^-, Ca^{2+} and Rb^+ were used. All scattering factors were modified to account for anomalous dispersion.[18] The final structural parameters are listed in Table 1, and selected interatomic distances and angles are given in Table 2.

Table 2. Selected Interatomic Distances (Å) and Angles (deg)[a]

Framework	$Ca_{31}Rb_{30}$-X	$Ca_{28}Rb_{36}$-X
Si-O(1)	1.63(1)	1.64(1)
Si-O(2)	1.61(1)	1.67(1)
Si-O(3)	1.63(1)	1.68(1)
Si-O(4)	1.64(1)	1.62(1)
average	**1.63(1)**	**1.65(2)**
Al-O(1)	1.70(1)	1.70(1)
Al-O(2)	1.77(1)	1.67(1)
Al-O(3)	1.75(1)	1.72(1)
Al-O(4)	1.68(1)	1.68(1)
average	**1.73(1)**	**1.69(1)**
Ca(1)-O(3)	2.43(1)	2.41(1)
Ca(2)-O(2)	2.29(1)	2.31(1)
Rb(1)-O(2)	2.99(1)	2.99(1)
Rb(2)-O(2)	2.77(1)	2.81(1)
Rb(3)-O(1)	3.38(1)	3.39(1)
Rb(3)-O(4)	3.05(1)	2.97(1)
O(1)-Si-O(2)	110.2(7)	110.5(5)
O(1)-Si-O(3)	109.5(6)	107.9(5)
O(1)-Si-O(4)	110.7(6)	110.8(5)
O(2)-Si-O(3)	108.9(6)	107.7(4)
O(2)-Si-O(4)	104.7(6)	107.6(5)
O(3)-Si-O(4)	112.7(6)	112.3(5)
O(1)-Al-O(2)	111.7(6)	111.4(5)
O(1)-Al-O(3)	105.1(5)	105.5(5)
O(1)-Al-O(4)	113.3(6)	112.3(5)
O(2)-Al-O(3)	107.5(5)	107.7(4)
O(2)-Al-O(4)	104.5(6)	106.7(5)
O(3)-Al-O(4)	114.7(5)	113.2(5)
Si-O(1)-Al	125.4(7)	125.0(5)
Si-O(2)-Al	141.5(6)	143.5(5)
Si-O(3)-Al	130.6(6)	130.4(5)
Si-O(4)-Al	163.4(7)	163.4(6)
O(3)-Ca(1)-O(3)	93.3(3)	93.6(3)
O(2)-Ca(2)-O(2)	119.5(5)	119.7(4)
O(2)-Rb(1)-O(2)	82.8(4)	83.8(2)
O(2)-Rb(2)-O(2)	91.1(4)	90.6(3)
O(1)-Rb(3)-O(1)	133.4(4)	132.9(3)
O(4)-Rb(3)-O(4)	65.3(4)	65.3(3)

[a]Numbers in parentheses are estimated standard deviations in units of the least significant digit given for the corresponding value.

Discussion

Zeolite X is a synthetic counterpart of the naturally occurring mineral faujasite. The polyhedron with 14 vertices known as the sodalite cavity or β cage may be viewed as the principal building block of the aluminosilicate framework of the zeolite (see Figure 1). These β-cages are connected tetrahedrally at 6-rings by bridging oxygens to give double 6-rings (D6R's, hexagonal prisms), and, concomitantly, an interconnected set of even larger cavities (supercages) accessible in three dimensions through 12-ring (24-membered) windows. The Si and Al atoms occupy the vertices of these polyhedra. The oxygen atoms lie approximately half-way between each pair of Si and Al atoms, but are displaced from those points to give near tetrahedral angles about Si and Al.

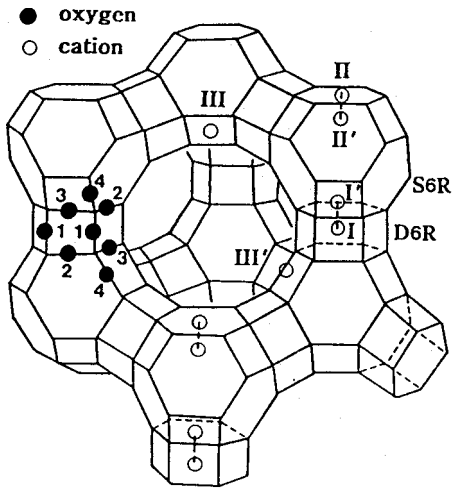

Figure 1. A stylized drawing of the framework structure of zeolite X. Near the center of the each line segment is an oxygen atom. The different oxygen atoms are indicated by the numbers 1 to 4. Silicon and aluminum atoms alternate at the tetrahedral intersections, except that Si substitutes for about 4% of the Al's. Extraframework cation positions are labeled with Roman numerals.

The nomenclature of the cation sites is as follows: site I, at the center of a D6R; site II, at the center of the single 6-ring (shared by a β- and a supercage), or displaced from this point into a supercage; sites I' and II' lie in the sodalite cavity, on opposite sides of the corresponding 6-rings from sites I and II, respectively; and site III, on a twofold axis opposite a 4-ring inside the supercage.

$Ca_{31}Rb_{30}$-X. In this structure, Ca^{2+} ions and Rb^+ ions are found at six different crystallographic sites. Thirty-one Ca^{2+} ions occupy two crystallographic sites and about thirty Rb^+ ions found at three such sites.

The Ca^{2+} ions at Ca(1) fill the 16-fold site I. Each Ca^{2+} ion at Ca(1) is octahedrally coordinated by O(3) framework oxygens (Ca(1)-O(3)=2.43(1) Å, O(3)-Ca(1)-O(3) angle=93.3 (3)°) (see Figure 2). About 19.0 Ca^{2+} ions at Ca(2) occupy the 32-fold site II in the supercage. The Ca(2)-O(2) distance, 2.29 Å, is a little shorter than the sum of the conventional radii[14] of Ca^{2+} and O^{2-}, 0.99 Å+1.32 Å=2.31 Å, presumably because Ca(2) is only three-coordinate. These Ca^{2+} ions are slightly recessed, 0.25(1) Å, into the supercage from the plane of the three O(2) oxygens (see Tables 2 and 3). The O(2)-Ca(2)-O(2) bond angle, 119.5(5)°, is nearly trigonal planar.

The Rb(1) position is at site II', on a threefold axis inside the sodalite unit at the single six-oxygen ring (see Figure 4). This is 32-fold position, but it is occupied by only 2 Rb^+ ions. Each Rb^+ ion lies relatively far inside the sodalite cavity, 1.99 Å from the plane of the three O(2) framework

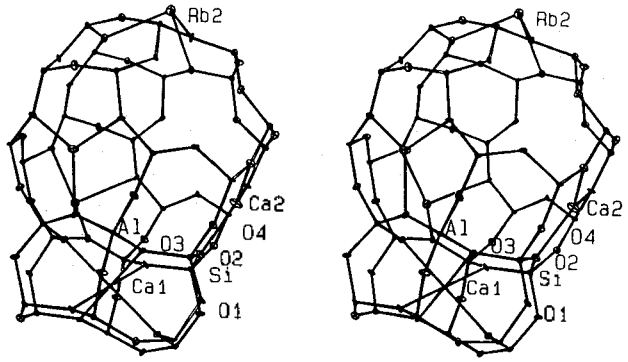

Figure 2. Stereoview of a representative sodalite cavity and D6R in dehydrated $Ca_{31}Rb_{30}$-X. All D6R's are filled as shown with Ca^{2+} ions at Ca(1). About 87.5% of the sodalite cavities have two Ca^{2+} ions at Ca(2) and two Rb^+ ions at Rb(2); the remainder have one Ca^{2+} ion at Ca(2), two Rb^+ ions at Rb(1) and one Rb^+ ion at Rb(2). Ellipsoids of 20% probability are shown.

Table 3. Deviations (Å) of Cations from 6-Ring Planes

	$Ca_{31}Rb_{30}$-X	$Ca_{28}Rb_{36}$-X
at O(3)[a]		
Ca(1)	−1.32(1)	−1.30(1)
at O(2)[b]		
Ca(2)	0.25(1)	0.16(1)
Rb(1)	−1.99(1)	−1.88(1)
Rb(2)	1.60(1)	1.60(1)

[a] A negative deviation indicates that the atom lies in the sodalite unit. [b] A positive deviation indicates that the atom lies in the supercage.

oxygens. The Rb(1)-O(2) distances are 2.99(1) Å, longer than the sum of the corresponding ionic radii, 1.47+1.32=2.79 Å.[14]

The Ca(2), Rb(1), and Rb(2) ions occupy site II in the supercage with occupancies of 15, 2, and 15, respectively, filling this 32-fold equipoint. Ca(2)-O(2) is 2.29(1) Å and O(2)-Ca(2)-O(2)=119.3(5)°; Rb(1)-O(2)=3.20(1) Å and O(2)-Rb(1)-O(2)=76.3(3); Rb(2)-O(2) is 2.99(1) Å and O(2)-Rb(2)-O(2) is 82.5(3)°. The fourteen Ca^{2+} ions at Ca(2) are only 0.19 Å from the plane of the single 6-ring; the ten Rb^+ ions at Rb(2) are much further, 1.94 Å, from the corresponding plane. Plausible ionic arrangements for a sodalite unit and a supercage are shown in Figures 2 and 3, respectively.

The remaining sixteen Rb^+ ions occupy the 48-fold Rb(3) position at site III (see Figure 3). The Rb(2)-O(4) approach distance, 3.11(1) Å, is longer than the sum of ionic radii of Rb^+ and O^{2-}, 1.47 Å+1.32 Å=2.79 Å,[14] which indicates that these ions are loosely held to the framework oxygens.

Recently the crystal structures of Cd_{46}-X,[19] Ba_{46}-X,[20] Ca_{46}-X,[21] Mg_{46}-X,[22] and K_{92}-X[5] were determined (see Table 3). From these it appears that site I (at the center of the D6R) is the lowest energy site for most cations, except for the largest and the smallest. Ca^{2+} ions in Ca_{46}-X and Cd^{2+} ions in Cd_{46}-X fill site I, with the remainder going to site II in the supercage, nearly filling it. About thirteen Ba^{2+} ions in

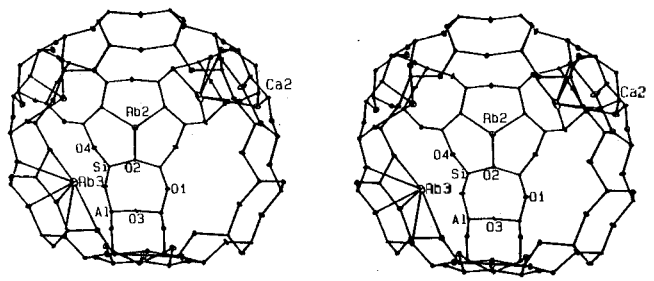

Figure 3. A stereoview of the supercage of dehydrated $Ca_{31}Rb_{30}$-X. Two Ca^{2+} ions at Ca(2), two Rb^+ ions at Rb(2) and two Rb^+ ions at Rb(3) are shown. About 63% of the supercages may have this arrangement. About 25% of supercages may have two Ca^{2+} ions at Ca(2), two Rb^+ ions at Rb(2) and one Rb^+ ion at Rb(3). The remainder may have one Ca^{2+} ion at Ca(2), two Rb^+ ions at Rb(1), one Rb^+ ion at Rb(2), and one Rb^+ ion at Rb(3). Ellipsoids of 20% probability are shown.

Table 4. Distribution of Nonframework Atoms over Sites

Crystals / Sites	$Ca_{31}Rb_{30}$-X	$Ca_{28}Rb_{36}$-X
I	16 Ca(1)	16 Ca(1)
II'	2 Rb(1)	4 Rb(1)
II	15 Ca(2)	12 Ca(2)
	15 Rb(2)	16 Rb(2)
III	13 Rb(3)	16 Rb(3)

Ba_{46}-X and fourteen Mg^{2+} in Mg_{46}-X occupy the sixteenfold site I position.[20]

Considerations of ionic size and charge govern the competition for sites in $Cd_{24.5}Tl_{43}$-X.[19] The smaller and more highly charged Cd^{2+} ions select their sites "first" because they can approach the anionic oxygens of the zeolite framework more closely. They nearly fill the site I position, with the remainder going to site II as in Cd_{46}-X, affirming that Cd^{2+} ions prefer site I, the D6R sites. Only after the Cd^{2+} ions have selected their sites do the Tl^+ ions finish filling site II, with the remainder going to the least suitable cation site in the structure, site III.

$Ca_{28}Rb_{36}$-X. Twenty-eight Ca^{2+} ions occupy two crystallographic sites and about thirty-six Rb^+ ions found at three such sites. About 16.0 Ca^{2+} ions at Ca(1) fill the 16-fold site I. Cations with Pauling radii much greater than 1.25 Å should not be able to replace the Na^+ ions in the D6R's;[23] the approximate value of 1.17 Å is suitable for comparison with the non-Pauling radii[14] used throughout this report. The radii of the Ca^{2+} and Rb^+ ions are 0.99 Å and 1.47 Å, respectively,[14] so site I should be accessible only to Ca^{2+}. Proof of this comes from the crystal structure of the partially Rb^+-exchanged zeolite X in which site I remains entirely unoccupied.[9] Each Ca(1) is octahedrally coordinated by O(3) framework oxygens at 2.41(1) Å (see Figure 4).

The Rb(1) position is at site II', on a threefold axis inside the sodalite unit at the single six-oxygen ring. (see Figure 4). This is 32-fold position, but it is occupied by only 4 Rb^+ ions. Each Rb^+ ion lies relatively far inside the sodalite cavity, 1.88 Å from the plane of the three O(2) framework

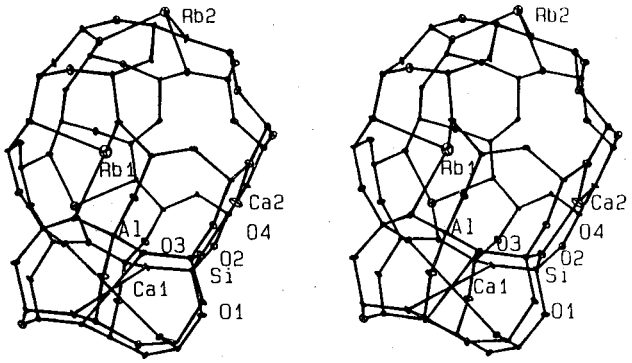

Figure 4. Stereoview of a representative sodalite cavity and D6R in dehydrated $Ca_{28}Rb_{36}$-X. All D6R's are filled as shown with Ca^{2+} ions at Ca(1). About 50% of the sodalite cavities have one Ca^{2+} ion at Ca(2), one Rb^+ ion at Rb(1) and two Rb^+ ions at Rb(2); the remainder have two Ca^{2+} ions at Ca(2) and two Rb^+ ions at Rb(2). Ellipsoids of 20% probability are shown.

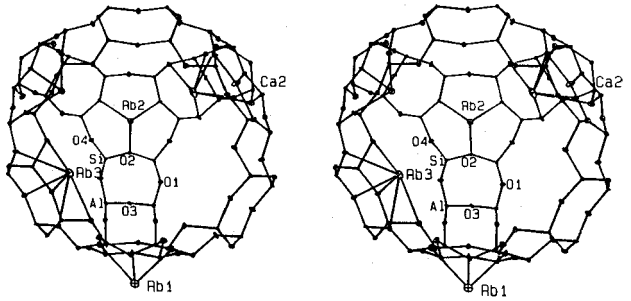

Figure 5. A stereoview of the supercage of dehydrated $Ca_{28}Rb_{36}$-X. One Ca^{2+} ion at Ca(2), one Rb^+ ion at Rb(1), two Rb^+ ions at Rb(2), and two Rb^+ ions at Rb(3) are shown. About 50% of the supercages may have this arrangement. The remainder may have two Ca^{2+} ions at Ca(2), two Rb^+ ions at Rb(2), and two Rb^+ ions at Rb(3). Ellipsoids of 20% probability are shown.

oxygens. The Rb(1)-O(2) distances are 2.99(1) Å, longer than the sum of the corresponding ionic radii, 1.47+1.32=2.79 Å.[14]

The Ca(2), Rb(1), and Rb(2) ions occupy site II in the supercage with occupancies of 12, 4, and 16, respectively, completely filling this 32-fold equipoint. Ca(2)-O(2) is 2.31(1) Å and O(2)-Ca(2)-O(2)=119.7(4)°; Rb(1)-O(2)=2.99(1) Å and O(2)-Rb(1)-O(2)=83.8(2); Rb(2)-O(2) is 2.81(1) Å and O(2)-Rb(2)-O(2) is 90.6(3)°. The twelve Ca^{2+} ions at Ca(2) are only 0.19 Å from the plane of the single 6-ring; the two Rb^+ ion lies relatively far inside the sodalite cavity, 1.88 Å from the plane of the three O(2) framework oxygen; the ten Rb^+ ions at Rb(2) are much further, 1.60 Å, from the corresponding plane. Plausible ionic arrangements for a sodalite unit and a supercage are shown in Figures 2, 3, and 4, respectively.

The remaining sixteen Rb^+ ions occupy the 48-fold Rb(3) position at site III (see Figure 5). The Rb(3)-O(4) approach distance, 2.97(1) Å, is the same as the sum of ionic radii of Rb^+ and O^{2-}, 1.47 Å+1.32 Å=2.79 Å.[14]

Conclusions

This work indicates that all of the Na^+ ions in zeolite X can readily be replaced by Ca^{2+} and Rb^+ ions. Ca^{2+} ions in both structures fill the apparently most favorable site I positions (at the D6R centers), with the remainder going to site II in the supercage, nearly half filling it. Considerations of ionic size and charge govern the competition for sites in both structures. The smaller and more highly charged Ca^{2+} ions nearly fill site I, with the remainder going to site II as in Ca_{46}-X[21], affirming that Ca^{2+} ions prefer site I. The larger Rb^+ ions, which are less able to balance the anionic charge of the zeolite framework because of their size, finish satisfying the sodalite cavity with some occupancy at II', and finish filling site II, with the remainder going to the least suitable cation site in the structure, site III. In both structures, no Rb^+ ions occupy site I. Rb^+ ion is apparently too large to occupy the center of the double 6-ring, when they are competing with other smaller cations like Ca^{2+} ions.

Acknowledgment. This work was supported in part by the Basic Research Institute Program, Ministry of Education, Korea, 1996, Project No. BSRI-96-3409.

References

1. Mortier, W. J. *Compilation of Extra-framework Sites in Zeolites*; Butterworth Scientific Ltd., Guildford, UK, 1982.
2. Schollner, R.; Broddack, R.; Kuhlmann, B.; Nozel, P.; Herden, H. Z. *Phys. Chem. (Leipzig)* **1981**, *262*, 17.
3. Egerton, T. S.; Stone, F. S. *J. Chem. Soc., Faraday Trans. I* **1970**, *66*, 2364.
4. Calligaris, M.; Mezzetti, A.; Nardin, G.; Randaccio, L. *Zeolites* **1986**, *6*, 137.
5. Calligaris, M.; Mezzetti, A.; Nardin, G.; Randaccio, L. *Zeolites* **1985**, *5*, 317.
6. Pluth, J. J.; Smith, J. V.; Mortier, W. J. *Mater. Res. Bull.* **1977**, *12*, 1001.
7. Bresciani-Pahor, N.; Calligaris, M.; Narin, G.; Randaccio, L.; Russo, E.; Comin-Chiaramonti, P. *J. Chem. Soc., Dalton Trans.* **1980**, 1511.
8. Smolin, Y. I.; Shepelev, Y. F.; Anderson, A. A. *Acta Crystallogr.*, Sect B **1989**, *45*, 124.
9. Shepelev, Y. F.; Butikova, I. K.; Smolin, Yu. I. K.; Smolin, Yu. I. *Zeolite* **1991**, *11*, 287.
10. Jang, S. B.; Song, S. H.; Kim, Y. *J. Korean Chem. Soc.* **1995**, *39*, 7.
11. Bogomolov, V. N.; Petranovskii, V. P. *Zeolites* **1986**, *6*, 418.
12. Calculations were performed with *Structure Determination Package Programs*, ***MolEN***, Enraf-Nonius, Netherlands, 1990.
13. Kim, Y.; Han, Y. W.; Seff, K. *J. Phys. Chem.* **1993**, *97*, 12663.
14. *Handbook of Chemistry and Physics*, 70th ed., The Chemical Rubber Co., Cleveland, Ohio, 1989/1990, p F-187.
15. *International Tables for X-ray Crystallography*, Vol. II, Kynoch Press: Birmingham, England, 1974, p 302.

16. Cromer, D. T. *Acta Crystallogr.* **1965**, *18*, 17.
17. *International Tables for X-ray Crystallography*, Vol. IV, Kynoch Press, Birmingham, England, 1974, pp 73-87.
18. Reference 17, pp 149-150.
19. Kwon, J. H.; Jang, S. B.; Kim, Y.; Seff, K. accepted *J. Phys. Chem.* (will be printed in July).
20. Jang, S. B.; Kim, Y. *Bull. Korean Chem. Soc.* **1995**, *16*, 248.
21. Jang S. B.; Song, S. H.; Kim, Y. *J. Korean Chem. Soc.* **1995**, *39*, 7.
22. Yeom, Y. H.; Jang, S. B.; Song, S. H.; Kim. Y.; Seff K. submitted to *J. Phys. Chem.*
23. Sherry, H. S. *J. Phys. Chem.* **1968**, *72*, 12.

Study on the Development of CVD Precursors I-Synthesis and Properties of New Titanium β-Diketonates

Sung Taeg Hong†, Jong Tae Lim, Joong Cheol Lee‡, Ming Xue#, and Ik-Mo Lee*

Department of Chemistry, Inha University, Inchon 402-751, Korea
†Korea Testing and Research Institute for Chemical Industry, Seoul 150-038, Korea
‡Daejung Laboratory, Inchon, Korea
Received March 25, 1996

Preparation and properties of potential CVD (Chemical Vapor Deposition) precursors for the TiO_2, a major component of the perovskite materials such as PT, PLT, PZT, and PLZT were investigated. Reactions between β-diketones and $TiMe_3$, formed in situ failed to produce stable Ti(β-diketonate)$_3$ complexes but a stable purple solid, characterized as $(OTi(BPP)_2)_2$ (BPP=1,3-biphenyl-1,3-propanedione) was obtained when BPP was used. Several new $Ti(Oi\text{-}Pr)_2$(β-diketonate)$_2$ complexes with aromatic or ring substituents were synthesized by the substitution reaction of $Ti(OiPr)_4$ by β-diketones and characterized with ^{1}H NMR, IR, ICP, and TGA. Solid complexes such as $Ti(Oi\text{-}Pr)_2(BAC)_2$ (BAC=1-phenyl-2,4-pentanedione), $Ti(Oi\text{-}Pr)_2(BPP)_2$, $Ti(Oi\text{-}Pr)_2(1\text{-}HAN)_2$ (1-HAN=2-hydroxy-1-acetonaphthone), $Ti(Oi\text{-}Pr)_2(2\text{-}HAN)_2$ (2-HAN=1-hydroxy-2-acetonaphthone), $Ti(Oi\text{-}Pr)_2(ACCP)_2$ (ACCP=2-acetylcyclopentanone), and $Ti(Oi\text{-}Pr)_2(HBP)_2$ (HBP=2-hydroxybenzophenone) were found to be stable toward moisture and air. $Ti(Oi\text{-}Pr)_2(ACCP)_2$ and $Ti(Oi\text{-}Pr)_2(HBP)_2$ were proved to have lower melting points and higher decomposition temperatures. However, these complexes are thermally stable and pyrolysis under an inert atmosphere resulted in incomplete decomposition. $Ti(Oi\text{-}Pr)_2(DPM)_2$ (DPM=dipivaloylmethane) and $Ti(Oi\text{-}Pr)_2(HFAA)_2$ (HFAA=hexafluoroacetylacetone) were sublimed substantially during the thermal decomposition. Pyrolysis mechanism of these complexes are dependent on type of β-diketone but removal of Oi-Pr ligands occurs before the decomposition of β-diketonate ligands.

Introduction

Recent development in the information and communication industries demands higher density of dynamic random access memory (DRAM) than ever and it is becoming a concensus that this goal can be achieved only by introducing higher dielectric materials such as $SrTiO_3$ or (Ba, Sr)TiO_3.[1] Moreover, Lead titanate ($PbTiO_3$) based ceramics such as PT, PZT, PLZT and PLT were found to have interesting piezoelectric, pyroelectric, ferroelectric, and electrooptic properties which can be applicable to nonvolatile ferroelectric RAMs, optoelectronic devices, sensors, and transducers.[2] Metal organic chemical vapor deposition (MOCVD) has been investigated as a promising technique for the commercial production of thin films of these ceramics, especially for the better step coverage, easy scale-up, easy control of composition and thickness, and limited diffusion of substrate while many processing techniques are available.[3] The success of this technique requires reliable precursors of high volatility, low toxicity and high stability. Several precursors such as metal alkyls and alkoxides have been used for their volatility but their toxicity and instability toward temperature, moisture and other chemicals limited wider uses. On the other hand, metal β-diketonates are stable toward hydrolysis and temperature, moderately volatile and nontoxic. In the above perovskite structure materials, TiO_2 is a major component and several alkoxide-based precursors such as $Ti(OEt)_4$,[2b,4] $Ti(Oi\text{-}Pr)_4$,[1b,5] and $Ti(Ot\text{-}Bu)_4$[5a] have been used as a thin film precursor but some disadvantages such as moisture sensitivity, step coverage, and possible intermolecular reactions amongst several precursors in the process of transportation in the CVD chamber were pointed out even though these are quite volatile. For the purpose of improving these properties of the precursors, new precursors such as $Ti(DPM)_2Cl_2$, $Ti(Oi\text{-}Pr)_2(DPM)_2$,[6] and $TiO(DPM)_2$[1b] were employed. These compounds were chosen for all source materials to have a similar reaction velocity and diffusion coefficient. This may help to have even distribution of composition along the carrier gas flow direction. However, no systematic investigation on the effect of substituents of β-diketonates on the physical properties

*Post Doctoral Fellow in Inha University (1995-1996).